Applied Physics
Express

LETTER • OPEN ACCESS

High-quality 100% Ce^{3+}:$(Lu_{1-x}Y_x)_2SiO_5$ single crystals grown by the hydrothermal technique

To cite this article: Encarnación G. Víllora *et al* 2024 *Appl. Phys. Express* **17** 122007

OPEN ACCESS

Applied Physics Express 17, 122007 (2024) LETTER

https://doi.org/10.35848/1882-0786/ad9b6c

High-quality 100% Ce^{3+}:$(Lu_{1-x}Y_x)_2SiO_5$ single crystals grown by the hydrothermal technique

Encarnación G. Víllora[1†*], Makoto Saito[2], and Kiyoshi Shimamura[1†*]

[1]National Institute for Materials Science, 1-1 Namiki, Tsukuba, Ibaraki, 305-0044, Japan
[2]Mitsubishi Chemical Corp., 1000 Kamoshida, Yokohama, Kanagawa, 227-8502, Japan

*E-mail: VILLORA.Garcia@nims.go.jp and SHIMAMURA .Kiyoshi@nims.go.jp

†These authors contributed equally to this work.

Received November 29, 2024; revised December 5, 2024; accepted December 6, 2024; published online December 23, 2024

The growth of Ce:$(Lu_{1-x}Y_x)_2SiO_5$ single crystals by the hydrothermal technique is demonstrated. Crystallographic defects are suppressed thanks to the growth at much lower temperatures, and therefore, the complete incorporation of cerium in the Ce^{3+} valence state is obtained. The growth under supercritical water lowers the temperature to less than half the melting point. In contrast, crystals grown from melt by the standard Czochralski technique possess intrinsic defects and undesirable Ce^{4+} ions as charge compensators. The growth of large-size single crystals with improved scintillation properties at a low cost is envisaged. © 2024 The Author(s). Published on behalf of The Japan Society of Applied Physics by IOP Publishing Ltd

Ce-doped lutetium oxyorthosilicate crystals, Lu_2SiO_5 (LSO) and $(Lu_{1-x}Y_x)_2SiO_5$ (x>0) (LYSO), are considered to be the best scintillators for gamma-ray detection in positron emission tomography (PET) of nuclear medicine and in high-energy physics.[1–8)] They compromise relevant properties: a high density (ρ ~7 g cm^{-3}) and an effective atomic number (Z_{eff} ~66), resulting in a high stopping power ($\rho \cdot Z_{eff}^4$ ~140×10^6), a high light yield (LY) > 30,000 ph MeV^{-1}, a short decay time (~35 ns), and a high energy resolution (~8% @ 662 nm). Commercialization of these crystals started in the late 1990s, and since then, large efforts have been made to improve their performance further.[9–20)] Nowadays, mass production of 3- to 4-inch crystals is carried out by the Czochralski (Cz) technique, despite the expensive Lu_2O_3 raw material and, more particularly, the ultra-high cost of Ir crucibles.

The development of Ce:$(Lu_{1-x}Y_x)_2SiO_5$ (x≥0) (Ce:L(Y)SO) single crystals has been closely bound from the beginning with investigating the oxygen vacancies and the valence state of Ce, and subsequent co-doping approaches. Soon, it was found that annealing under an oxidizing atmosphere improves the scintillation LY, shortens the decay time, and decreases both the afterglow and the thermoluminescence, suggesting the presence of oxygen vacancies in as-grown crystals.[21–24)] While reducing the oxygen vacancy concentration, this oxidation process promotes a partial Ce valence change from trivalent to tetravalent, as the absorbance spectra indicate.[24,25)] Therefore, a positive trade-off was assumed between less deep traps, causing non-radiative recombination, and a slight decrease in activator Ce^{3+} concentration. Ce^{4+} cations have been considered undesirable because they lead to a broad charge transfer band (CTB) between oxygen 2p-orbitals of the valence band and Ce^{4+} 4f-orbitals within the bandgap (peaking at ~4.9 eV) that does not contribute to luminescence in UV excitation spectra of Ce:L(Y)SO crystals. However, this is not always the case, as demonstrated for Sr_2CeO_4 with Ce in the tetravalent state.[26,27)] Furthermore, Ce radioluminescence has been reported for 100% Ce^{4+}-doped silica glasses[28)] and annealed Ce^{4+}:$Li_6Y(B_3O)_3$ single crystals.[29)]

By X-ray absorption near edge spectroscopy (XANES), the direct evidence of the Ce^{4+} presence has been pursued in Ce:L(Y)SO[24,25,30)] as well as in Ce:$Gd_3Ga_3Al_2O_{12}$ (Ce:GGAG)[31,32)] scintillators. Assuming a detection limit of 5%, the existence of Ce^{4+} in as-grown and annealed Ce:L(Y)SO crystals could not be found by XANES despite observing the CTB in absorbance spectra. Annealing can drastically increase the photo- and radioluminescence by 40% and 20%, respectively, while the CTB slightly enhances.[24)] In contrast, in the case of Ce:GGAG crystals, the Ce^{4+} concentrations estimated by XANES differ from non-detectable to 50%.[31,32)]

Beyond annealing, co-doping with divalent alkaline earth Ca^{2+} and Mg^{2+} cations has been demonstrated to improve the scintillation properties of Ce:L(Y)SO crystals significantly, even though it favors the incorporation of Ce in the tetravalent state.[8,25,33–36)] Ce^{4+} concentrations as high as 20% for Ce,Mg:LYSO and 35% for Ce,Ca:LYSO have been estimated by XANES upon small nominal codopant concentrations.[25)] It is assumed that Ce^{4+} ions act as charge compensators of intrinsic point defects, possibly the above-mentioned oxygen vacancies, so that original deep traps that lead to non-radiative recombination are suppressed. Furthermore, Ce^{4+} ions are suggested to contribute to radioluminescence in the same way as Ce^{3+} emitters upon gamma excitation when they capture relaxing electrons from the upper conduction bands. Actually, prior to emission, Ce^{3+} centers are required to be excited while Ce^{4+} ones are not. Instead, after emission, Ce^{4+} centers need to capture a hole while Ce^{3+} do not. Co-doping improves LY, decay time, and afterglow, but it has drawbacks such as spiral growth, the tendency of crystals to crack, uncontrolled doping, etc., which lead to a low production yield.[37)] As a solution, triple co-doping with divalent Zn^{2+} [15,38)] and tetravalent Si^{4+} and Zr^{4+} ions[33)] has been proposed.

To summarize, though Ce^{3+} is the ideal isovalent activator for L(Y)SO on Lu^{3+} sites,[39–41)] non-isovalent Ce^{4+} ions are always present since the CTB is systematically observed in Cz-grown crystals. These ions are a part of the charge compensators for intrinsic crystal defects, possibly oxygen

vacancies, that appear during the growth of oxides from melt at high temperatures. Though co-doping aids in suppressing non-radiative recombination centers, improving the general scintillation performance, it is not the ideal solution. The growth of defect-free crystals with Ce in the trivalent state is desirable. For this, a decrease in the growth temperature seems to be a prerequisite. Flux growth is a promising alternative to lower the growth temperature to avoid intrinsic defects created at high temperatures. The solvothermal one, particularly the hydrothermal (HT) under supercritical water, is proper for the growth of oxide crystals with higher melting points like Ce:L(Y)SO. As with quartz, large scaling could drastically reduce production costs while avoiding at the same time the use of expensive Ir crucibles.

In this study, we demonstrate the growth of undoped and Ce-doped LSO and Ce:LYSO single crystals by the HT technique. The optical characterization of grown crystals shows that the HT technique provides additional advantages beyond production costs, such as fewer crystal defects and full incorporation of Ce in the desired trivalent state. Furthermore, though the direct measurement of Ce in the tetravalent state has been elusive, the way to discriminate the presence of Ce^{4+} in low concentrations is elucidated.

Undoped and Ce-doped LSO and LYSO single crystals were grown with the HT technique using an autoclave. High-purity (4 N) Lu_2O_3, SiO_2, Y_2O_3 and CeO_2 were used as raw materials. The nominal concentration of Y relative to Lu was chosen as 10%, while the nominal concentration of Ce-doped crystals was fixed at 0.15% relative to (Lu +Y). Potassium hydroxide (KOH) was used as a mineralizer with a concentration in the water of approximately 20 M. Relatively high growth temperatures, in the range 630 °C to 730 °C, were needed to properly dissolve the raw materials in the supercritical fluid state. The reactor was heated for 12 hs, kept for 24 hs at the maximum temperature, and then cooled, first for several hours at 1 °C/h, then for 12 hs down to room temperature. Correspondingly, the used pressures were relatively high, typically ranging between 100 and 200 MPa. The reactions took place within sealed Ag-ampoules of 10 mm in length and 5 mm in diameter under a temperature gradient of about 50 °C.

To compare the new hydrothermal crystals with standard ones, an undoped LSO crystal was grown by the Cz-technique with a 30 kW generator. 4 N raw materials of Lu_2O_3 and SiO_2 (1 mol% enriched from the stoichiometric ratio to compensate for evaporation losses) were mixed and loaded in an Ir crucible. A 1-inch single crystal was grown under an Ar + 0.2% O_2 flow of 1 l min^{-1}. The rotation and pulling rates were 10 rpm and 1 mm h^{-1}, respectively. Furthermore, to investigate the Ce incorporation from the valence point of view a Ce:LYSO single crystal from Saint-Gobain was used for comparison.

The crystals' composition was measured by electron-probe-microanalysis (EPMA) using a JEOL JXA-8500F operated at 15 kV. Powder X-ray diffraction (XRD) measurements were carried out using a Rigaku SmartLab3 diffractometer with Cu Kα radiation (1.54059 Å). Transmittance spectra were recorded with a JASCO UV–vis-NIR spectrometer V-570. Excitation and photoluminescence (PL) spectra were acquired with a JASCO FP-8600DS fluorescence spectrometer.

By spontaneous nucleation single crystals of few mm in size were obtained reproducibly by the HT technique.

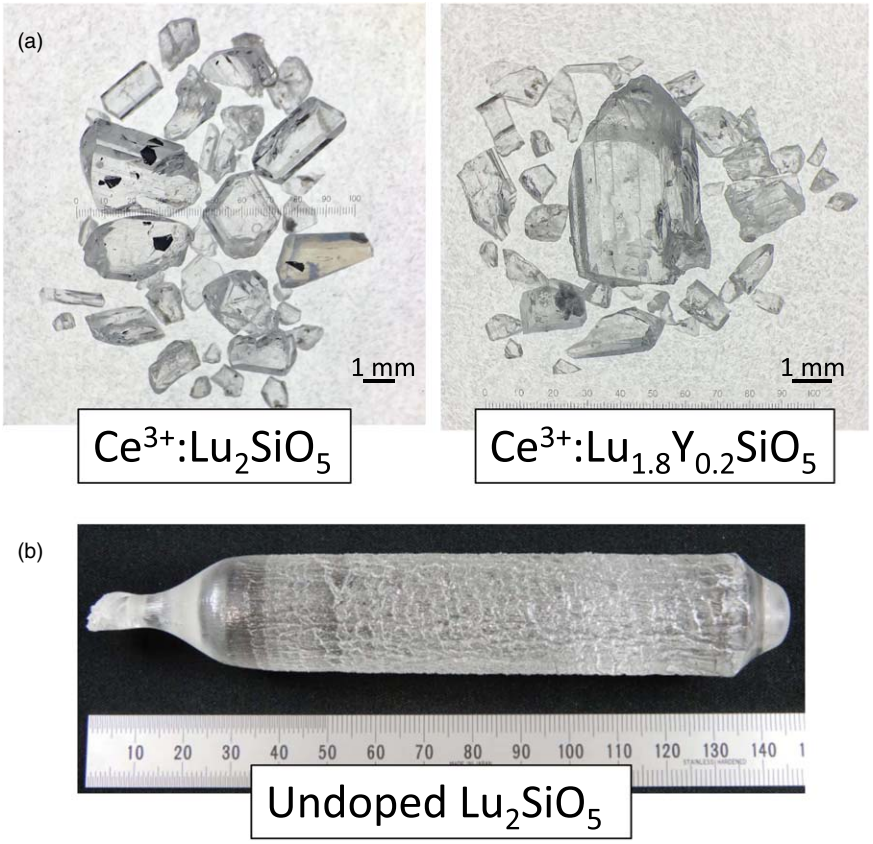

Fig. 1. (a) As-grown Ce^{3+}:LSO & Ce^{3+}:LYSO single crystals by the HT technique, and (b) 1-inch LSO single crystal grown by the Cz-technique.

As-grown Ce:LSO and Ce:LYSO single crystals are shown in Fig. 1(a) as an example. Through the smooth and faceted surfaces, it can be seen that the crystals are transparent, colorless, and without inclusions. On the contrary, the 1-inch undoped LSO single crystal grown by the Cz-technique exhibits a very rough surface, as can be seen in Fig. 1(b). Only after cutting and polishing, it could be confirmed that the crystal is transparent and colorless, free of cracks and inclusions from top to bottom.

The composition of all crystals was evaluated by EPMA. The results are given in Table I. The measured concentrations of Y and Ce in HT-grown crystals are very close to the nominal ones, suggesting that the segregation coefficients are very close to one for both cations. Instead, the Y and Ce concentrations in reference Ce:LYSO crystal grown by the Cz-technique are lower by approximately 1/2 and 1/3, respectively. The content of other elements within the experimental error is comparable for both growth techniques.

The crystallographic phase of grown crystals was evaluated by powder XRD. All grown crystals exhibit the monoclinic phase with space group C12/c1. For example, the diffraction pattern of HT LSO is depicted in Fig. 2, together with the corresponding simulation. The difference between HT- and Cz-grown crystals becomes evident during the optical characterization in the ultraviolet UV wavelength region, first by comparing the undoped crystals, and then the doped ones.

The UV transmittance spectra of undoped LSO crystals grown by HT- and Cz-technique are shown in Fig. 3. Both crystals exhibit a high transparency above 250 nm. Below, towards the absorption cutoff, the Cz-grown crystal presents an obvious, though shallow, broad absorption band. The origin of this band is assumed to be related to point defects, caused by growth at high temperatures (the melting point of LSO is 2047 °C), when SiO_2 evaporates strongly from the melt and some oxygen deficiency can be expected. On the contrary, as the HT crystal was grown at a much lower temperature, less than half, the formation of such intrinsic defects could be entirely suppressed. Therefore, no optical losses are observed in the whole transparent region. This advantage of HT growth can be extrapolated to Ce-doped crystals, though it is not evident due to the overlap of Ce absorption bands in the UV wavelength region.

For doped crystals, the UV transmittance spectra of HT-grown Ce:LSO and Ce:LYSO are shown together with the spectrum of Cz-grown Ce:LYSO reference in Fig. 4(a). Both HT-grown crystals present four well-defined absorption bands ascribed to the parity-allowed electric dipole $4f^1 \rightarrow 5d^j$ (j = 1–4) intraatomic Ce^{3+} transitions. The absorption intensities are very close for both HT-grown crystals, in good accordance with the nominally equal Ce concentration. In contrast, the Cz-grown Ce:LYSO crystal exhibits a lower $4f^1 \rightarrow 5d^1$ absorption, due to the lower Ce concentration as found by EPMA, and not well-resolved higher energy absorption bands. The absorption spectra were calculated using the well-known Bouguer–Lambert–Beer law and deconvoluted to gain more insight. The absorption spectra of HT-grown crystals are described very well by the five Gaussian curves, as shown for the case of Ce:LSO in Fig. 4(b), with peak maxima at 3.47, 3.80, 4.20, 4.69, and 5.90 eV (i.e. 357, 326, 295, 264, and 210 nm), in good accordance with the reported deconvolution.[42] This result suggests that all Ce is incorporated as Ce^{3+} in HT crystals, and is further supported by the deconvolution of Cz crystal in Fig. 4(c). Taking into account the relative intensities of Ce^{3+} absorption bands in HT crystals, the absorption of Cz-grown Ce:LYSO is composed of the Ce^{3+} intraatomic absorption bands, with a 1/3 intensity of that of HT-grown Ce:LSO, in good agreement with EPMA results, and a very broad absorption band starting at about 3.5 eV (354 nm) and going beyond 6 eV, overlapping with the conduction band. This absorption, with the maximum at ~4.9 eV, is generally attributed to the CTB of the Ce^{4+}-O^{2-}

Table I. Relative cationic concentrations of single crystals measured by EPMA; recalculated to a total sum of three, like in the chemical formula.

Cation	CZ LSO	CZ Ce:LYSO	HT LSO	HT Ce:LSO	HT LYSO	HT Ce:LYSO
Lu	1.920	1.820	1.903	1.921	1.729	1.744
Si	1.080	1.098	1.097	1.076	1.100	1.095
Y	—	0.081	—	—	0.171	0.158
Ce	—	0.001	—	0.002	—	0.003

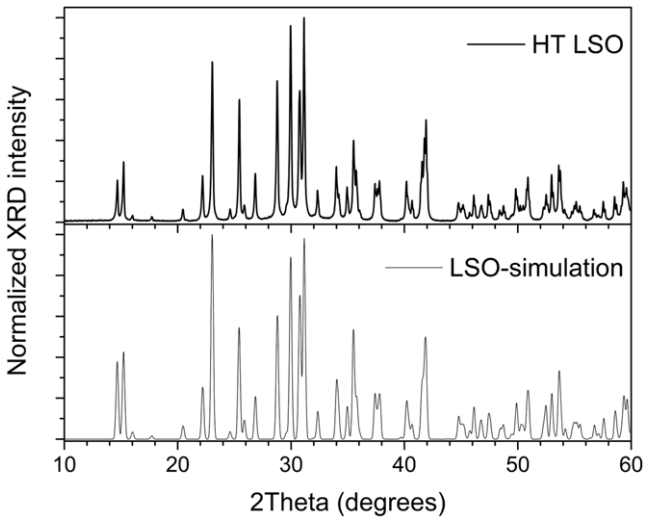

Fig. 2. Powder XRD pattern of HT-grown LSO single crystal compared with LSO simulation.

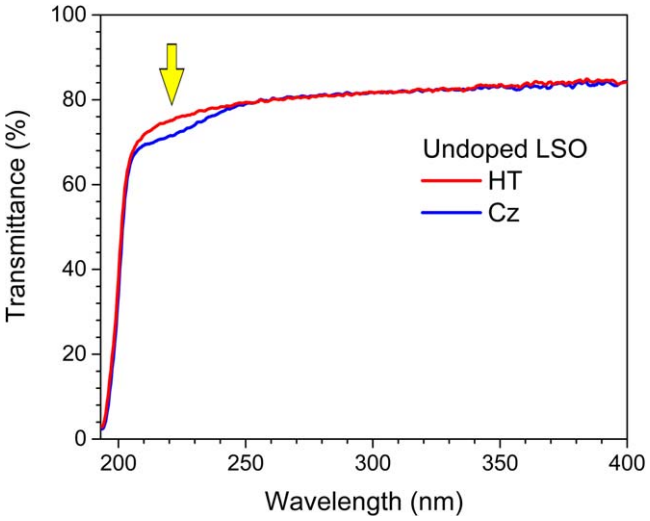

Fig. 3. Transmittance of undoped HT- and Cz-grown LSO single crystals in the UV wavelength region.

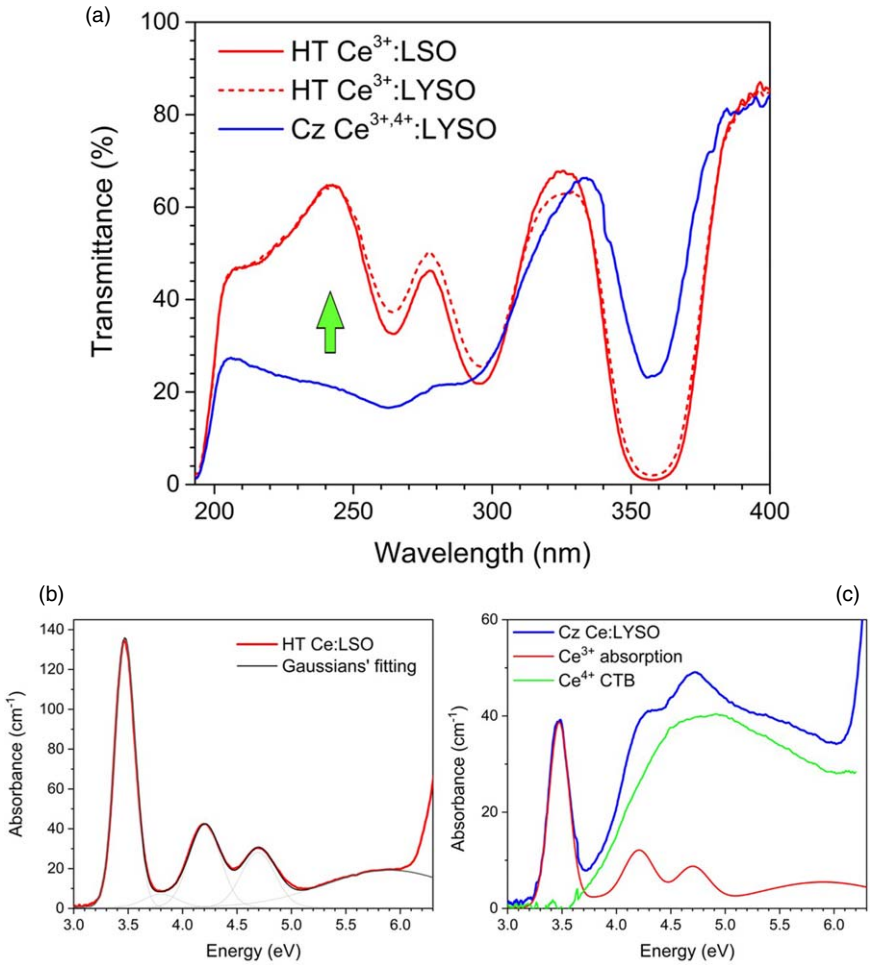

Fig. 4. (a) Transmittance of Ce-doped single crystals: HT-grown Ce:LSO & Ce:LYSO and Cz-grown Ce:LYSO reference. Deconvolution of absorbance spectra of (b) HT-grown Ce:LSO and (c) Cz-grown Ce:LYSO single crystals.

centers. The location of the CTB varies with the host material and is non-symmetric, consisting of at least three absorption bands.[27,43] Additionally, in contrast to Ce^{3+}, the absorption cross-section of the Ce^{4+} CTB is unknown in scintillator crystals. As the estimated absorption cross-section ratio Ce^{4+}/Ce^{3+} for Ce-doped glasses points out a significant difference, ~5[44] and ~16,[45] it is reasonable to assume that this ratio could be approximately one order of magnitude larger in scintillators. This would explain why the presence of Ce^{4+} can be easily detected by transmittance measurements in scintillator crystals with low Ce^{4+} concentrations, and observing and quantifying Ce^{4+} in the XANES measurements, that are used as standard, is difficult. Furthermore, the influence of CTB absorption is also observed in the PL measurements.

Figure 5 shows the excitation and emission PL spectra of Ce-doped crystals and the photograph of HT-grown Ce:LSO upon UV excitation. Both HT-grown crystals exhibit almost overlapping curves due to similar Ce concentrations, as with the transmittance curves of Fig. 4(a). The intensity ratios at the wavelength maxima 354:294:264 are as high as 1:0.84:0.61 and 1:0.77:0.60 for HT-grown Ce:LSO and Ce:LYSO, respectively, which contrasts with the low 1:0.31:0.22 ratios in Cz-grown Ce:LYSO. The excitation spectra of HT crystals look like the absorption spectra, indicating that all the UV absorption occurs only on Ce^{3+} ions. On the contrary, the excitation and absorption spectra of the Cz-grown Ce:LYSO crystal barely resemble each other below 350 nm, where the CTB occurs. Photons absorbed at the Ce^{4+}-O^{2-} centers do not contribute to PL emission, and therefore, the $4f^1 \rightarrow 5d^j$ (j = 2,3) excitation peaks are much smaller than the main $4f^1 \rightarrow 5d^1$ one. This phenomenon is observed systematically in the reported PL spectra of commercial scintillators.[3] Therefore, lower intensities in the upper excitation bands can be used as an additional signature of the presence of undesirable Ce^{4+} ions. At last, it should be noted that all crystals present approximately the same emission spectra, except for the small differences caused by Y mixing. The spectra are characterized by a double peak broad emission from the lowest upper state to the ground states of Ce^{3+}, namely $5d^1 \rightarrow 4f^1$ ($^2F_{5/2}$ and $^2F_{7/2}$). The PL of HT-grown crystals upon UV excitation is homogeneous and bright, as shown in the photograph of Fig. 5(b). Larger-sized crystals will be grown for the light yield determination in the near future.

The growth of undoped and Ce-doped LSO and LYSO crystals by the HT technique is demonstrated. The advantages over the standard Cz-technique are, on the one hand, higher crystal perfection due to a much lower growth temperature and, on the other hand, complete incorporation of Ce in the trivalent state Ce^{3+}, thus paving the way for a breakthrough in scintillation performance. The elimination of various defects is of crucial importance for the suppression of non-radiative recombination processes and, therefore, for the

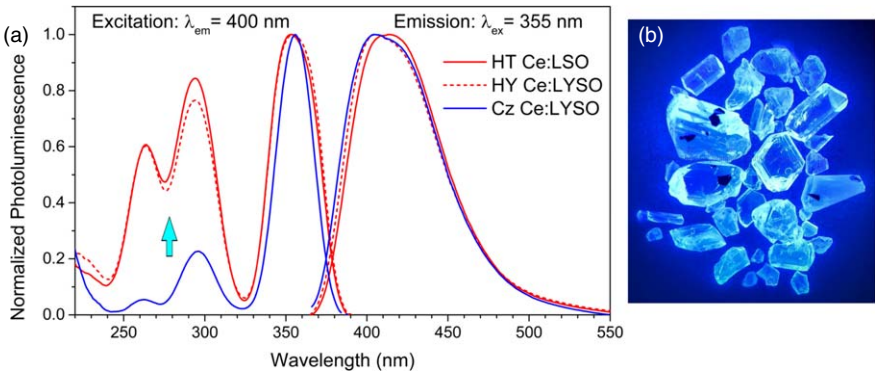

Fig. 5. (a) Normalized excitation and emission PL spectra of Ce-doped crystals: HT-grown Ce:LSO & Ce:LYSO and Cz-grown Ce:LYSO reference. (b) Photograph of the HT-grown Ce:LSO crystals upon 365 nm lamp excitation.

improvement of scintillation properties in terms of light yield, decay time, and afterglow. Currently applied co-doping approaches become superfluous, and instead, a revision of the optimal Ce concentration is necessary. Furthermore, as expensive Ir crucibles are no longer needed and upscaling autoclaves for the growth of large-size single crystals is straightforward, the production cost can be drastically reduced. Therefore, this study lets us envisage the development of Ce^{3+}:LSO & Ce^{3+}:LYSO single crystals with an improved scintillation performance at a much lower cost.

1) C. W. E. van Eijk, Phys. Med. Biol. **47**, R85 (2002).
2) C. M. Pepin, P. Bérard, A-L. Perrot, C. Pépin, D. R. Lecomte, C. L. Melcher, and H. Dautet, IEEE Trans. Nucl. Sci. **51**, 789 (2004).
3) J. Chen, R. Mao, L. Zhang, and R-Y. Zhu, IEEE Trans. Nucl. Sci. **54**, 718 (2007).
4) R-Y. Zhu, J. Phys. Conf. Ser. **587**, 012055 (2015).
5) R-Y. Zhu, J. Phys. Conf. Ser. **928**, 012015 (2017).
6) T. Yanagida, Proc. Jpn. Acad., Ser. B **94**, 75 (2018).
7) P. Lecoq et al., Phys. Med. Biol. **65**, 21RM01 (2020).
8) F. M. Addesa et al., JINST **17**, P08028 (2022).
9) M. Kapusta, M. Moszynski, M. Balcerzyk, J. Braziewicz, D. Wolski, J. Pawelke, and W. Klamra, IEEE Trans. Nucl. Sci. **47**, 1341 (2000).
10) A. Syntfeld-Kažuch, M. Moszyński, Ł. Świderski, T. Szczęśniak, A. Nassalski, C. L. Melcher, M. A. Spurrier, B. Goliszek, P. Kamiński, and M. Nowaczyk, IEEE Trans. Nucl. Sci. **56**, 2972 (2009).
11) V. Jarý, M. Nikl, E. Mihóková, J. A. Mareš, P. Průša, P. Horodyský, W. Chewpraditkul, and A. Beitlerová, IEEE Trans. Nucl. Sci. **59**, 2079 (2012).
12) N. G. Starzhinskiy, O. T. Sidletskiy, G. Tamulaitis, K. A. Katrunov, I. M. Zenya, Y. V. Malyukin, O. V. Viagin, A. A. Masalov, and I. A. Rybalko, IEEE Trans. Nucl. Sci. **60**, 1427 (2013).
13) V. Kalinnikov and E. Velicheva, Phys. Part. Nucl. Lett. **11**, 259 (2014).
14) F. Yang, R. Mao, L. Zhang, and R-Y. Zhu, Nucl. Instrum. Methods Phys. Res. A **784**, 105 (2015).
15) C. L. Melcher et al., JPS Conf. Proc. **11**, 020001 (2016).
16) E. Auffray et al., Phys. Status Solidi a **215**, 1700798 (2018).
17) Y. Wu, M. Tian, J. Peng, M. Koschan, I. Greeley, C. Foster, and C. L. Melcher, Phys. Status Solidi RRL **13**, 1800472 (2019).
18) G. Tamulaitis, E. Auffray, A. Gola, M. Korzhik, A. Mazzi, V. Mechinski, S. Nargelas, Y. Talochka, A. Vaitkevičius, and A. Vasil'ev, J. Phys. Chem. Solids **139**, 109356 (2020).
19) V. Kalinnikov, E. Velicheva, and Y. Uozumi, Phys. Part. Nucl. Lett. **18**, 457 (2021).
20) V. Nadig, K. Herweg, M. M. C. Chou, J. W. C. Lin, E. Chin, C-A. Li, V. Schulz, and S. Gundacker, Phys. Med. Biol. **68**, 075002 (2023).
21) B. Chai, U.S. Patent U.S.A.7,166,845 (2007).
22) B. Liu, Z. Qi, M. Gu, X. Liu, S. Huang, and C. Ni, J. Phys. Condens. Matter **19**, 436215 (2007).
23) D. Ding, H. Feng, G. Ren, M. Nikl, L. Qin, S. Pan, and F. Yang, IEEE Trans. Nucl. Sci. **57**, 1272 (2010).
24) S. Blahuta, A. Bessière, B. Viana, V. Ouspenski, E. Mattmann, J. Lejay, and D. Gourier, Materials **4**, 1224 (2011).
25) S. Blahuta, A. Bessière, B. Viana, P. Dorenbos, and V. Ouspenski, IEEE Trans. Nucl. Sci. **60**, 3134 (2013).
26) L. Van Pieterson, S. Soverna, and A. Meijerink, J. Electrochem. Soc. **147**, 4688 (2000).
27) L. Li, S. Zhou, and S. Zhang, Chem. Phys. Lett. **453**, 283 (2008).
28) M. Fasoli, A. Vedda, A. Lauria, F. Moretti, E. Rizzelli, N. Chiodini, F. Meinardi, and M. Nikl, J. Non-Cryst. Solids **355**, 1140 (2009).
29) D. Yuan, E. G. Víllora, N. Kawaguchi, D. Nakauchi, T. Kato, T. Yanagida, and K. Shimamura, Jpn. J. Appl. Phys. **62**, 010614 (2023).
30) C. L. Melcher, S. Friedrich, S. P. Cramer, M. A. Spurrier, P. Szupryczynski, and R. Nutt, IEEE Trans. Nucl. Sci. **52**, 1809 (2005).
31) G. Dantelle, G. Boulon, Y. Guyot, D. Testemale, M. Guzik, S. Kurosawa, K. Kamada, and A. Yoshikawa, Phys. Status Solidi b **257**, 1900510 (2020).
32) Y. Wu, F. Meng, Q. Li, M. Koschan, and C. L. Melcher, Phys. Rev. Appl. **2**, 044009 (2014).
33) Y. D. Zavartsev, S. A. Koutovoi, and A. I. Zagumennyi, J. Cryst. Growth **275**, e2167 (2005).
34) M. A. Spurrier, P. Szupryczynski, K. Yang, A. A. Carey, and C. L. Melcher, IEEE Trans. Nucl. Sci. **55**, 1178 (2008).
35) K. Yang, C. L. Melcher, P. D. Rack, and L. A. Eriksson, IEEE Trans. Nucl. Sci. **56**, 2960 (2009).
36) W. Chewpraditkul, C. Wanarak, T. Szczesniak, M. Moszynski, V. Jary, A. Beitlerova, and M. Nikl, Opt. Mater. **35**, 1679 (2013).
37) S. Blahuta, K. Yang, V. Ouspenski, and P. Menge, Poster presented at IEEE Nucl. Sci. Symp. & Med. Imaging Conf. (Strasbourg, France), Oct. 29 - Nov. 5, 2016.
38) M. A. Spurrier, P. Szupryczynski, H. Rothfuss, K. Yang, A. A. Carey, and C. L. Melcher, J. Cryst. Growth **310**, 2110 (2008).
39) H. Suzuki, T. A. Tombrello, L. Melcher, and J. S. Schweitzer, IEEE Trans. Nucl. Sci. **40**, 380 (1993).
40) L. Pidol, O. Guillot-Noël, A. Kahn-Harari, B. Viana, D. Palenc, and D. Gourier, J. Phys. Chem. Solids **67**, 643 (2006).
41) D. W. Cooke, B. L. Bennett, K. J. McClellan, J. M. Roper, and M. T. Whittaker, Phys. Rev. B **61**, 11973 (2000).
42) V. A. Tedzhetov, A. V. Podkopaev, and A. A. Sysoev, IOP Conf. Series: Mater. Sci. Eng. **525**, 012044 (2019).
43) A. M. Efimov, A. I. Ignat'ev, N. V. Nikonorov, and E. S. Postnikov, Opt. Spectrosc. **111**, 426 (2011), Original Russian text published in Optika i Spektroskopiya 458.
44) M-L. Brandily-Anne, J. Lumeau, L. Glebova, and L. B. Glebov, J. Non-Cryst. Solids **356**, 2337 (2010).
45) A. M. Efimov, A. I. Ignatiev, N. V. Nikonorov, and E. S. Postnikov, J. Non-Cryst. Solids **361**, 26 (2013).